Talanta 256 (2023) 124315

Contents lists available at ScienceDirect

Talanta

journal homepage: www.elsevier.com/locate/talanta

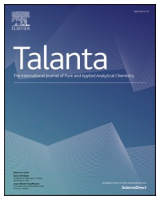

Extraction of selected benzothiazoles, benzotriazoles and benzenesulfonamides from environmental water samples using a home-made sol-gel silica-based mixed-mode zwitterionic sorbent modified with graphene

Alberto Moral [a], Francesc Borrull [a], Kenneth G. Fourton [b], Abuzar Kabir [b], Rosa Maria Marcé [a,*], Núria Fontanals [a]

[a] Universitat Rovira i Virgili, Department of Analytical Chemistry and Organic Chemistry, Sescelades Campus, Marcel·lí Domingo 1, 43007 Tarragona, Spain
[b] Florida International University, Department of Chemistry and Biochemistry, Miami, FL 33199, USA

ARTICLE INFO

Handling Editor: Kin-ichi Tsunoda

ABSTRACT

A novel sol-gel silica-based mixed-mode zwitterionic sorbent modified with graphene microparticles was synthesized. Thanks to the inclusion of multiple functional groups and graphene microparticles to exert a wide range of intermolecular/interionic interactions including dipole-dipole interactions, ion-exchange interactions and π-π interactions, the sorbent showed high retention in the solid-phase extraction (SPE) of benzothiazoles, benzotriazoles and benzenesulfonamides.

The SPE protocol was optimized in terms of pH, sample loading volume and elution conditions using liquid chromatography coupled to high resolution mass spectrometry (LC-HRMS). The method based on SPE followed by LC-HRMS was validated. Apparent recoveries at two levels of concentration were in the range from 48 to 85% (in most cases) in matrices such as influent wastewater, matrix effect was lower than ±30% in most cases, method detection and quantification limits being lower than 20 ng/L and repeatability and reproducibility between days were lower than 18% (n = 4).

River, effluent and influent wastewaters samples were analyzed, obtaining concentrations ranging from 3 to 175 ng/L in river samples, from 12 to 499 ng/L in effluent samples and from 15 to 632 ng/L in influent samples, when the compounds were above the method quantification limits.

1. Introduction

In recent years, benzotriazoles (BTRs), benzothiazoles (BTs) and benzenesulfonamides (BSAs) have been categorized as high production volume chemicals. BTRs are mainly used as UV blockers [1] or as corrosion inhibitors [2,3], BTs have a wide variety of industrial applications (vulcanization accelerators, fungicides, corrosion inhibitors or UV stabilizers) [4,5], and BSAs have also many applications such as plasticizers or intermediates in the synthesis of diverse products such as dyes or pesticides [4,6]. Their widespread use has compelled to consider them as emerging pollutants. These compounds have been determined not only in samples of environmental interest such as water [7–11], sludge [12] or particle matter [13,14] but also in fish [15], urine [16], clothes [17,18] and tea beverages [19] among others. Their ubiquitous occurrence has led to evaluate the toxicity effects, for instance, the effect of the exposition to BTs and BTRs has been studied in several vertebrates, mainly fishes [20,21] but also in humans [14,22,23]. Meanwhile, there are less studies about the toxicity of the BSAs [24–26].

From the structural point of view, BTRs, BTs and BSAs are highly heterogeneous groups of compounds. BTRs and BTs are based on a benzene ring fused with a five-member heterocycle which for the BTRs is a 1,2,3-triazole ring and for the BTs is a 1,3-thiazole ring. BSAs are based on a benzene ring with a sulfonamide group. Depending on the functionalization, the physicochemical characteristics of these compounds are broadly dispersed and far apart from each other, for instance, benzothiazole has a pK_a of 0.9, meanwhile their "amino" and the "hydroxy" derivatives have pK_a values of 3.9 and 10.4, respectively.

One way to determine these compounds in liquid samples is to use

* Corresponding author.
E-mail address: rosamaria.marce@urv.cat (R.M. Marcé).

https://doi.org/10.1016/j.talanta.2023.124315
Received 7 November 2022; Received in revised form 26 January 2023; Accepted 28 January 2023
Available online 31 January 2023

solid-phase extraction (SPE) followed by chromatographic techniques with mass spectrometry detection, which allow low levels to be quantified in analyzed samples [6,7,9,27,28]. One of the most common option is to use polymer reversed-phase sorbents in SPE, such as the Oasis HLB sorbent commercialized by Waters [6,7]. However, the search for more selective methods and the ability to perform ionic interactions have led to the use of commercial mixed-mode ion-exchange sorbents because they combine reversed-phase and ionic interactions [11,29] or the combination of mixed-mode ion-exchange sorbents (Strata X-AW and X–CW) with reversed phase sorbents (Isolute ENV+) [28]. Moreover, the development of home-made sorbents with high π delocalized density to perform π-π interactions has been also explored [9].

As have been mentioned, the group of BTs, BTRs and BSAs cluster a wide variety of compounds. Ideally, they can be retained through cationic, anionic, and reversed-phase interactions [11], so a sorbent which combines these three interactions could be of interest. Mixed-mode zwitterionic sorbents combine reversed-phase interactions with both ionic interactions. Currently, this kind of sorbents cannot be acquired commercially, so the sorbents reported in literature are homemade. They can be polymer- [30,31] or silica-based [32,33]. Silica is an interesting substrate for sorbents because the reactivity of the silanol groups in the network allows for a wide variety of functional moieties to be introduced. And, in the recent years, the introduction of carbonaceous nanomaterials has been explored [34]. In this regard, the use of fullerenes, carbon nanotubes or graphene has been evaluated [35]. Graphene has a rich π delocalized density, high surface area, excellent thermal stability, and corrosion resistance, which make it particularly suitable to be used in novel sorbent development.

This study evaluates a novel mixed-mode zwitterionic sorbent. It is based on a sol-gel silica derived network where graphene microparticles are embedded and functionalized to simultaneously perform anionic, cationic, reversed-phase and π-π interactions. The sorbent was evaluated for the retention of a group of BTs, BTRs and BSAs, since they form a heterogeneous group having compounds that can be retained through cationic, anionic, reversed phase and π-π interactions. After being optimized for SPE, the sorbent was used to extract these compounds in river, effluent wastewater, and influent wastewater samples followed by liquid chromatography coupled to high resolution mass spectrometry (LC-HRMS) determination.

2. Experimental

2.1. Reagents and standards

The reagents used for sol-gel mixed-mode zwitterionic sorbent were tetramethyl orthosilicate (TMOS), methyl trimethoxysilane (MTMS), isopropanol (IPA), trifluoroacetic acid (TFA), hydrogen peroxide, methylene chloride, ammonium hydroxide and sulphuric acid. All of them were purchased from Sigma Aldrich (St. Louis, MO, USA).

3-mercaptopropyl trimethoxysilane (3-MPTMS), octadecyl trimethoxysilane (C_{18}-TMS), and N-trimethoxysilyl propyl N,N,N-trimethyl ammonium chloride (N-TMPTMAC) were acquired from Gelest Inc. (Morrisville, WI, USA).

Ultrapure water was provided by a water purification system (Millipore, Burlington, USA), HPLC grade methanol (MeOH) and acetonitrile (ACN), and MS grade MeOH, ACN and water were purchased from Carlo Erba (Val de Reuil, France). Acetic acid (HAc), formic acid and hydrochloric acid were purchased from Sigma-Aldrich.

Solid standards of 1-H-benzotriazole (BTR), 4-methyl-1-benzotriazole (4TTR), 5-methyl-1-benzotriazole (5TTR), 5,6-dimethyl-1-benzotriazole (XTR), 5-chloro-1-H-benzotriazole (ClBTR), benzothiazole (BT), 2-hydroxybenzothiazole (OHBT), 2-(methylthio)-benzothiazole (MeSBT), benzenesulfonamide (BSA), o-toluenesulfonamide (o-TSA), p-toluenesulfonamide (p-TSA), N-methyl-p-toluenesulfonamide (Me-p-TSA) and N-ethyl-p-toluenesulfonamide (Et-p-TSA) were purchased from Sigma Aldrich. Stock solutions of individual standards were prepared in MeOH at a concentration of 1000 mg/L and stored at −20 °C. The working solutions were prepared weekly in a mixture of ultrapure water and methanol (80/20, v/v) and were stored at 4 °C in brown bottles in the dark.

2.2. Synthesis of sol-gel mixed-mode zwitterionic sorbent with encapsulated graphene particles

The sol-gel mixed-mode zwitterionic sorbent was prepared using a facile sol-gel synthesis protocol developed in our laboratory. The sol solution for the sorbent was created by sequentially adding and subsequently vortexing of the building blocks tetramethyl orthosilicate (TMOS), methyl trimethoxysilane (MTMS), octadecyl trimethoxysilane (C_{18}-TMS), N-trimethoxysilyl propyl N,N,N-trimethyl ammonium chloride (N-TMPTMAC), 3-mercaptopropyl trimethoxysilane (3-MPTMS), isopropanol (IPA) and trifluoroacetic acid (TFA, 0.1 M) in a 50 mL centrifuge tube. The relative ratios of the ingredients (TMOS, MTMS, 3-MPTMS, C_{18}-TMS, N-TMPTMAC, IPA, and TFA) were maintained at 1: 1: 0.1: 0.1: 0.2: 3.8: 3, respectively. The mixture was vortexed for 5 min and subsequently sonicated for 15 min in order to eliminate any trapped air bubbles potentially present in the sol solution. The sol solution was kept at room temperature for 8 h to allow the sol-gel precursors to be completely hydrolyzed.

In a batch of approximately 65 mL sol solution, 0.1 g of graphene micro particles (5–10 μm) were added, and solution was sonicated for 30 min to obtain a near-homogenous dispersion of graphene particles.

Freshly prepared ammonium hydroxide (1 M) was then added in droplets to the hydrolyzed sol solution containing dispersed graphene microparticles under continuous stirring in a magnetic stirrer. The solution was seen to become viscous before turning into solid gel. The solid gel was aged and thermally conditioned at 60 °C for 48 h. The monolithic bed of the sol-gel network embedded with graphene micro particles was then pulverized and dried at 80 °C for 24 h and the sol-gel sorbent was broken into fine particles in a ball mill and rinsed with MeOH:methylene chloride (50:50, v/v) under sonication for 30 min. The particles were dried with air and treated with 30% H_2O_2 (with 0.1 M sulphuric acid) for 4 h. The sorbent particles were subsequently washed with deionized water several times and finally dried at 80 °C for 12 h. A detail process flow diagram for synthesizing sol-gel zwitterionic multimode sorbent with embedded graphene particles is presented in Fig. 1. The sol-gel zwitterionic mixed-mode sorbent with embedded graphene particles were then ready for using it for SPE.

2.3. Structure of sol-gel mixed-mode zwitterionic sorbent

The characterization of the sorbent was performed with a JEOL JSM 5900LV Scanning Electron Microscope (SEM) equipped with EDS-UTW detector, JEOL USA, Inc. (Peabody, MA, USA) for recording SEM images and a Cary 670 FTIR Spectrometer (Agilent Technologies, Santa Clara, CA, USA) for the Fourier Transform Infrared Spectroscopy (FT-IR).

The sorbent evaluated was named SiO_2-G-SAX/SCX (Fig. 1). It is based on silica modified with graphene microparticles and functionalized with C_{18} chains (reversed phase interactions), quaternary amines (strong anionic interactions, SAX) and sulfonic groups (strong cationic interactions, SCX). Moreover, the graphene microparticles allow to perform π-π interactions.

2.4. Solid-phase extraction procedure

A 10 μm polyethylene frit (Symta, Madrid, Spain) was fitted in an empty 6 mL SPE cartridge (Symta), to which 200 mg of the sorbent was added. Another 10 μm polyethylene frit was placed above the sorbent.

The SPE procedure was carried out in a SPE manifold (Teknokroma, Barcelona, Spain) connected to a vacuum pump. The sorbent was conditioned with 5 mL of MeOH and 5 mL of ultrapure water adjusted to

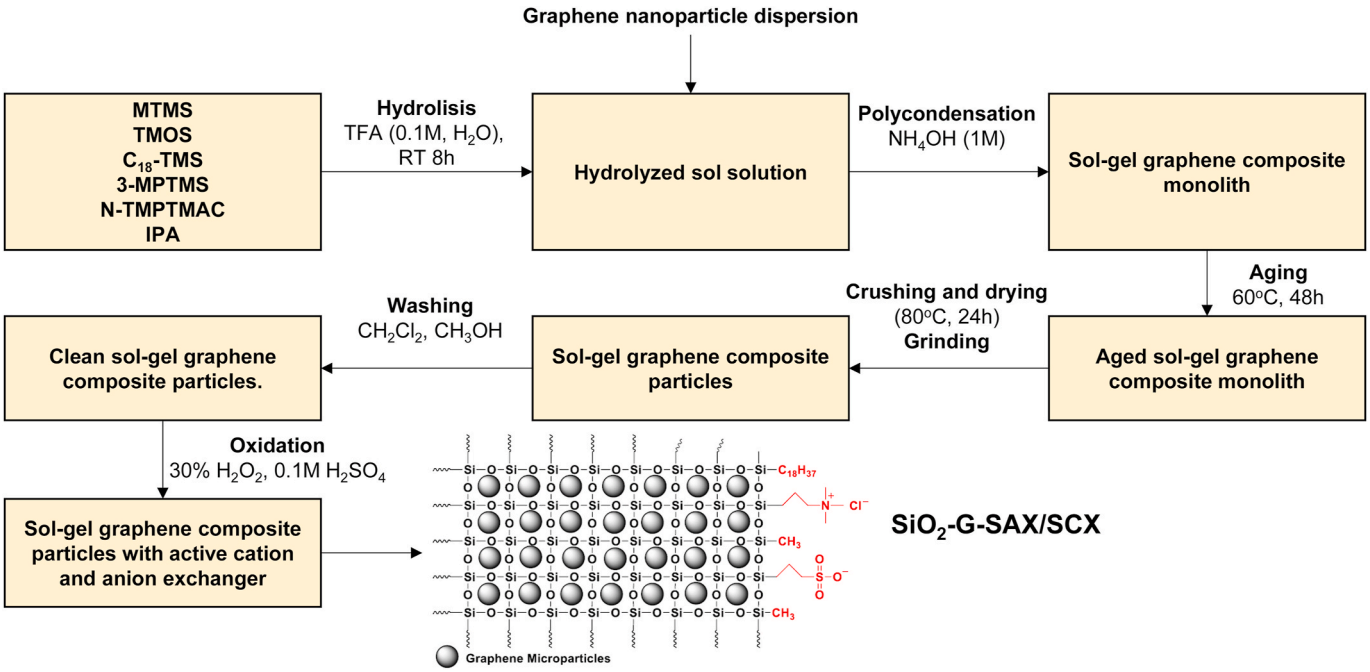

Fig. 1. Process flow diagram for synthesizing sol-gel multi-mode graphene composite sorbent.

pH 3, and then 100 mL of river water or 50 mL of influent and effluent wastewater adjusted to pH 3 with HCl were loaded into the cartridge at an approximately flow rate of 10 mL/min. Elution was carried out with 5 mL of MeOH. The eluted volume was evaporated with a miVac Duo centrifuge evaporator (Genevac, Ipswich, UK) to an approximate volume of 150 μL and reconstituted to 1 mL with initial mobile phase solution. The reconstituted extracts were filtered with 0.45 μm PTFE (polytetrafluoroethylene) syringe filters (Scharlab) before the analysis. To reuse the SPE cartridges, they were washed with 5 mL of MeOH and then they were completely dried by applying vacuum for 10 min. The reusability of the cartridges was evaluated up to 20 times, showing good precision.

Before analysis, all samples were filtered through a 0.45 μm nylon membrane filter (Scharlab). Effluent and influent samples were previously filtered with a 1.2 μm glass-fibre membrane filter (Fisherbrand, Loughborough, UK).

2.5. Liquid chromatography – high resolution mass spectrometry

Chromatographic analysis was carried out with an Accela 1250 UHPLC system from Thermo Scientific (Bremen, Germany) equipped with an automatic injector (Accela Autosampler) and a quaternary pump. The LC system was coupled to an Exactive Orbitrap mass spectrometer from Thermo Scientific equipped with a heated electrospray ionization (HESI) source and a high-energy collision dissociation (HCD) cell that fragmented the analytes for their confirmation. The chromatographic column used was Acquity UPLC HSS T3 (100 mm × 2.1 mm, 1.8 μm particle size) acquired from Waters (Milford, MA, USA).

The mobile phase was a mixture of 0.1% HCOOH in H_2O/ACN 98/2, v/v (solvent A) and MeOH (solvent B). The gradient profile started with 0% of B, and was increased to 20% in 8 min, when %B was held for 2 min before being increased to 25% in the next 5 min. Finally, %B was increased to 100% in the next 6 min, held for 3 min and then returned to the initial conditions in 1 min where it was held for 3 min. The flow rate was 400 μL/min, the column oven temperature was 50 °C and the injection volume was 20 μL.

The optimal parameters in positive ionization mode were: sheath gas flow rate, 40 arbitrary units (AU); auxiliary gas flow rate, 20 AU; sweep gas, 0 AU; spray voltage, 4 kV; capillary voltage, 37.5 V; tube lens voltage, 85 V; and skimmer voltage 20 V. The optimal parameters in negative ionization mode were: sheath gas flow rate, 45 AU; auxiliary gas flow rate, 15 AU; sweep gas, 0 AU; spray voltage, 4 kV; capillary voltage, −25 V; tube lens voltage, −90 V; and skimmer voltage −25 V. In both cases, the capillary temperature was 350 °C and the heater temperature was 400 °C. The compounds measured in positive mode were: BT, OHBT, MeSBT, BTR, 5TTR, 4TTR, ClBTR, XTR, Me-p-TSA and Et-p-TSA. The compounds measured in negative mode were BSA and TSA.

Four windows were used for data acquisition, two in negative mode (0–5.75 min and 8.50–10.10) and two in positive mode (5.75–8.50 and 10.10–22). In every window, two alternative scan events were set with a range of 50–250 *m/z*. The first event was a full scan at 50,000 FWHM with an injection time of 250 ms. The second scan was a fragmentation scan at 10,000 FWHM with an injection time of 50 ms and a collision voltage of 30 eV in the HCD in all windows. For quantification, the molecular ions were measured (with a mass extraction window of 5 ppm) and the selected fragments were used for confirmation. Table S1 shows the mass of the selected ions and their fragments.

2.6. Validation parameters

The method was validated in terms of recovery, matrix effect, linear range, method detection and quantification limits, repeatability and reproducibility between days.

SPE recovery (%R_{SPE}) and apparent recovery (%R_{app}) were used to evaluate the yield of the extraction. %R_{SPE} was obtained by analyzing standard solutions and was the recovery of the extraction. %R_{app} was obtained by analyzing spiked environmental water samples and was the recovery of the extraction considering the matrix effect. In both cases, the recovery was calculated as the ratio of the theoretical concentration and the concentration in LC-HRMS. In the case of the environmental water samples, the blank concentration was subtracted.

The matrix effect (%ME) was obtained using the formula: %ME = (C_e/C_t x 100) – 100, where "C_e" is the concentration obtained by spiking a blank sample after SPE and "C_t" is the expected concentration. A positive value indicates that the signal is enhanced while a negative value indicates that it is suppressed.

The linear range was tested with external calibration curves which analyzed seven solutions with different concentrations in triplicate. The method detection limit (MDL) was obtained as the concentration that

had a signal-to-noise ratio higher than 3 with one of the fragments providing a signal higher than 10^3, and the method quantification limit (MQL) was the lowest point from the calibration curves, accomplishing also a signal-to-noise ratio higher than 10.

Repeatability was obtained as the %RSD (relative standard deviation) (n = 4) by analysing spiked samples on the same day. The reproducibility between days was obtained as the %RSD by analyzing spiked samples (n = 4) on different days.

3. Results and discussion

3.1. Synthesis of the sol-gel mixed-mode zwitterionic graphene embedded sorbents

Sustainability and healthy progress of sorptive extraction and microextraction techniques primarily depend on the continuous influx of novel sorbents with improved selectivity, chemical and thermal stability. Carbonaceous particles including graphene oxide, graphene, activated carbon, carbon nanotubes have been found very promising in developing new sorbent materials. Graphene and graphene oxide are frequently used in both the extraction (e.g., solid-phase extraction) and microextraction (e.g., solid-phase microextraction) techniques [36]. Although graphene oxide, due to its possession of abundant hydroxide and carboxylic acid functional groups, are favoured in many applications, in the current project we used pristine graphene particles to increase the overall surface area so that the sample matrix can easily permeates through the composite sorbents and the analytes interact easily with different functional moieties implanted into the sol-gel matrix, resulting in faster extraction kinetic and higher extraction recovery. Graphene complements the other ingredients of the sol solution, methyl trimethoxysilane, octadecyl trimethoxysilane, 4-trimethoxysilylpropyl-N,N,N-trimethyl ammonium chloride and 3-mercaptopropyl trimethoxysilane to end with a sol-gel mixed-mode zwitterionic graphene embedded sorbent named SiO_2-G-SAX/SCX.

3.2. Characterization of sol-gel mixed-mode zwitterionic graphene embedded sorbents

Sol-gel mixed-mode zwitterionic graphene embedded sorbents were characterized using FT-IR and SEM-EDS to understand the chemical makeup, surface morphology and the elemental chemical composition. FT-IR spectra provides important information regarding the functional composition of the building blocks and their successful integration into the final sol-gel composite material. SEM images as well as the data obtained from Energy Dispersive X-ray Spectroscopy provide information regarding the surface morphology, apparent particle sizes and their distribution as well the elemental composition of the composite material.

3.2.1. Fourier Transform Infrared Spectroscopy (FT-IR)

The FT-IR spectra of the major component of graphene and the sol-gel sorbent with embedded graphene are presented in Supplementary Figure S1 and Fig. 2, respectively. All FT-IR spectra were presented over a range between 3000 and 700 cm $^{-1}$ at a resolution 4 cm^{-1}. Unlike graphene oxide, graphene does not possess different functional sites and therefore not many distinct features. FT-IR spectra of pristine graphene FT-IR spectra (Fig. 1S) has a broad and weak peak at ~1608 cm^{-1} that can be assigned to C═C stretching. The peak at ~2343 cm^{-1} corresponds to CO_2, suggesting incomplete reduction of graphene oxide during the manufacturing process of graphene [37]. The peak at ~1470 cm^{-1} may be attributed to C–H bending vibration. The FT-IR spectra of SiO_2-G-SAX/SCX (Fig. 2) maintained the signature peaks that appeared in pristine graphene spectra (Fig. S1). In addition, the peak at ~1037 cm^{-1} can be assigned to CO stretching vibration of Si–O–CH_3. Due to the very high content of graphene in the sol-gel matrix, the spectral contributions of other two major ingredients, 3-mercaptopropyl trimethoxysilane (3-MPTMS) and 4-(trimethoxysilylethyl) benzyl trimethyl ammonium chloride (4-TMSEBTMAC) were not recognized.

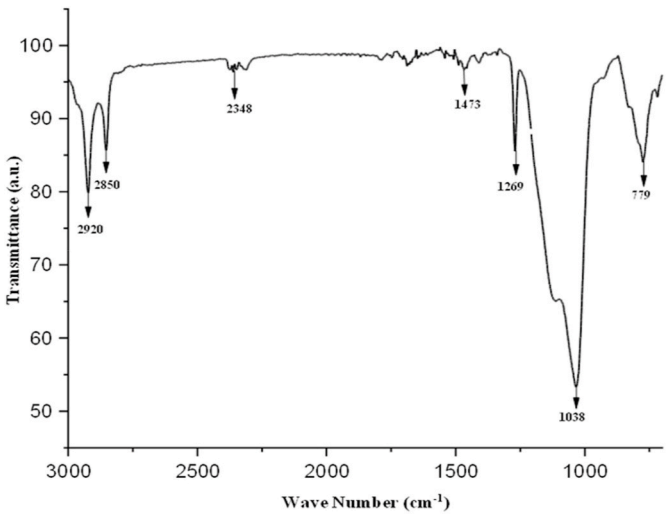

Fig. 2. FT-IR spectra of sol-gel graphene SAX/SCX sorbent.

3.2.2. Scanning electron Microscopy-Energy Dispersive X-ray spectroscopy

The surface morphology and the elemental composition of the sorbent was investigated using a SEM-EDS. The SEM images are presented in Fig. 3 (a, b) at 500x and 1,000x magnifications, respectively. The EDS images are presented in Fig. 3 (c, d). The SEM images showed that the particle sizes are not homogeneously distributed and have irregular shapes. Majority of the particles are in the range of 1–10 μm and of irregular shape. The broad distribution of particles helps them packing well for SPE with minimal void volume. The surface of the particles apparently looks rough that may augment the interaction between the particles and the analytes during the extraction process. The EDS data revealed the elemental composition of the sorbent with 35% Si, 32% O and 33% C. Due to the two sources of carbon, C_{18}-TMS and graphene in the sol solution, carbon appears to be a dominant component in the composite sorbent.

3.3. LC-HRMS conditions

Before evaluating the sorbent towards the selected group of compounds, the LC-HRMS conditions were settled. The challenge of the chromatographic optimization was the separation of two pairs of isomers: 4TTR and 5TTR and o-TSA and p-TSA. In order to separate 4TTR and 5TTR, solvent A initially consisted of 0.1% HCOOH in H_2O, but the compounds were not completely separated. Therefore, 2% of ACN was added [27], which made the separation satisfactory. However, the separation of the TSA isomers was not achieved under optimal conditions for the other compounds. So, they were determined as a mixture named TSA. This has also been reported in other studies [7,11,27].

In the HRMS, the signals were acquired in both positive and negative mode to optimize the signal of each analyte. This optimization was performed in full scan at high resolution (50,000 FWHM) in a mass range of 50–500 *m/z*. All the ions were quantified with positive ionization except BSA and TSA (Table S1), which, in agreement with previous studies, were quantified with negative ionization to obtain the highest signal possible [7,11,27]. Calibration curves were obtained for each analyte, with the highest limit being 500 μg/L. The lowest limit, which was also the instrumental quantification limit (IQL), ranged between 0.5 and 1 μg/L, except for BSA and TSA, which showed low ionization yields that caused low signal and IQL values of 20 μg/L. The instrumental detection limits (IDL) ranged between 0.1 and 0.5 μg/L except for BSA and TSA (10 μg/L).

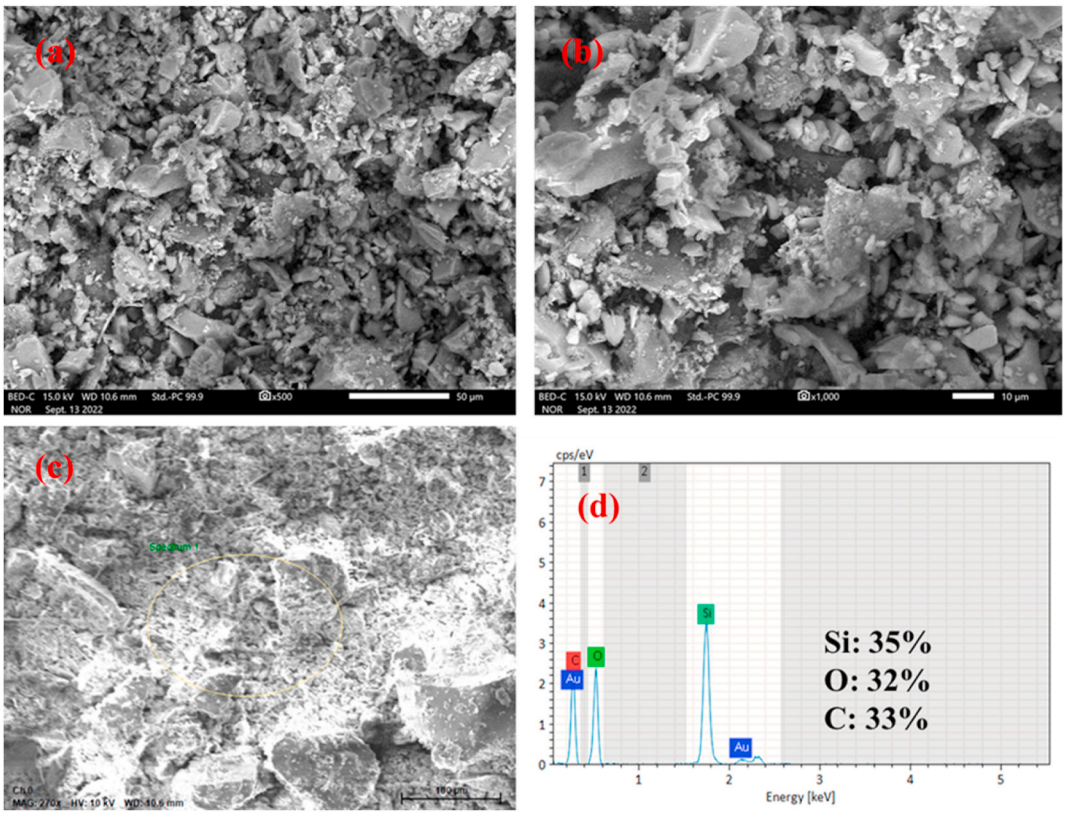

Fig. 3. SEM images of SiO_2-G-SAX/SCX particles (a) at 500x magnification; (b) at 1,000x magnification; (c) circled area used for EDS; (d) individual elemental spectra obtained from EDS.

3.4. Solid-phase extraction

Initially, the sorbent SiO_2-G-SAX/SCX was evaluated with standard solutions prepared in ultrapure water with all compounds at a concentration of 5 μg/L (except for BSA and TSA which was prepared at a concentration of 50 μg/L). The initial conditions were based on a previous study [32] which evaluated other home-made sol-gel silica-based mixed-mode zwitterionic sorbents: the loading volume was 25 mL of ultrapure water at pH 6, since there were a variety of pK_a compounds, and the elution step was 5 mL of 5% NH_4OH in MeOH and 5 mL of 5% HAc in MeOH.

As can be observed in Fig. 4, SiO_2-G-SAX/SCX presented SPE recoveries higher than 80% for all BTs and BTRs, and higher than 70% for the BSAs except for BSA whose $\%R_{SPE}$ was 40%. The sorbent was compared with two sorbents developed in a previous study [32] which had the same functionalization with C_{18} chains, quaternary amines, and sulfonic acids, but a silica network that was unmodified (SiO_2-SAX/SCX) or modified with carbon microparticles (SiO_2–C-SAX/SCX). As can be seen in Fig. 4, for most compounds the SPE recoveries of SiO_2-SAX/SCX and SiO_2–C-SAX/SCX are close to the ones obtained with SiO_2-G-SAX/SCX. However, the SPE recoveries for BTR, BSA and TSA were considerably higher and SiO_2-G-SAX/SCX showed that the inclusion of graphene microparticles improved performance.

In a previous study, Salas et al. [11] proposed that the delocalization

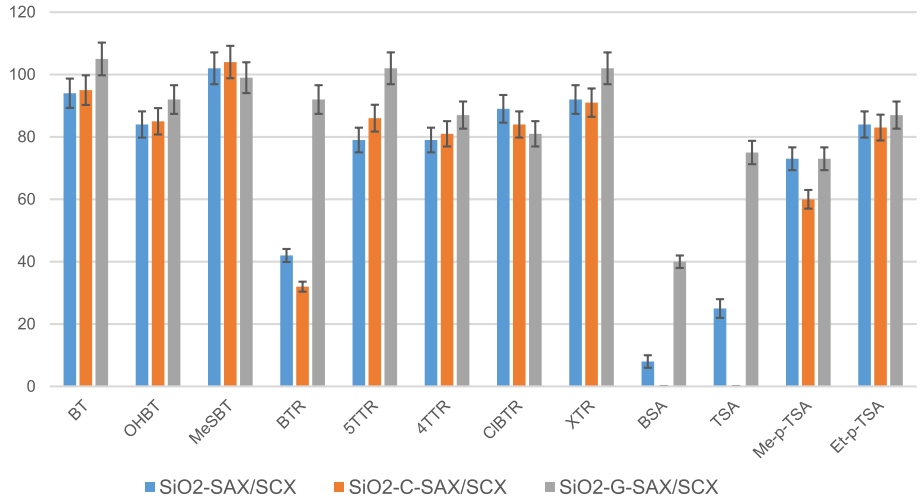

Fig. 4. Recoveries obtained when 25 mL of ultrapure water spiked at 5 μg/L were percolated with the different sorbents.

of charge between the fused rings in the BTs and the BTRs allows these compounds to interact through ionic exchange interactions. In our case, we exploited this electronic delocalization to interact with the graphene high π delocalized density, allowing SiO_2-G-SAX/SCX to present π-π interactions with these analytes. Moreover, BSAs have only one aromatic ring in their structures, so the delocalization is lower and there are fewer π-π interactions. Therefore, the SPE recoveries for these compounds were slightly lower than for BTs and BTRs.

To further improve the retention of the compounds, the pH was optimized by testing and comparing pH 3 and pH 6. As can be observed in Table 1, the SPE recoveries were slightly better at pH 3 for compounds like Me-p-TSA, so this pH was selected for the following tests. Some studies [11,27] that determined similar compounds using polymer-based sorbents such as Oasis HLB and Polyclean polymeric reported that the loading pH did not affect the $\%R_{SPE}$ of their compounds, whereas other studies [6,7,38] selected pH 3 for the loading solution.

To confirm that the compounds were retained through π-π interactions, a clean-up step was used to try to separate the compounds retained through hydrophobic and π-π interactions from the compounds retained through ionic interactions. The use of 1 mL of MeOH and 1 mL of a mixture of water and MeOH (1:1) was evaluated. In both cases, the compounds washed out in the clean-up step. In greater detail, the % of analytes eluted with the MeOH ranged from 35% (BSA) to 90% (Me-p-TSA). In the case of the mixture water:MeOH, the % lost in the clean-up step was slightly lower but was still too high, between 24% (XTR) and 75% (Et-p-TSA). These results confirmed that the compounds were mostly retained through hydrophobic and π-π interactions since they were rinsed with MeOH. Nonetheless, some studies did not include a clean-up when determining similar compounds [7,9,27].

Since the compounds were partially eluted with 1 mL of MeOH, the use of 5 mL of MeOH instead of a solution of NH_4OH in MeOH was evaluated. The $\%R_{SPE}$ eluting with 5 mL of MeOH ranged from 72% (TSA) to 98% (OHBT), except for BSA (54%) whose low retention has been mentioned above (Table 1). Therefore, this elution was selected. The use of MeOH to elute similar compounds has been reported in previous studies [7,9,27]. Of particular note is the study by Spelltini et al. [9] who modified silica with humic acids to determine BTs and BTRs. Humic acids made it possible for the sorbent to perform π-π interactions, as graphene did in the present study. They used 4 mL of MeOH to elute the compounds, which disrupted these interactions.

The increase in loading volume from 25 to 100 mL was evaluated with ultrapure water and no significant decrease was observed in the $\%R_{SPE}$. For 25 mL, values were between 77% and 92% (except BSA, 31%) and for 100 mL they were between 75% and 92% (except BSA, 33%) (Table S2). Thus, the optimized SPE procedure consisted of 100 mL of water adjusted to pH 3 for the loading step and 5 mL of MeOH for the elution step.

With these parameters, the $\%R_{SPE}$ was calculated by spiking ultrapure water at 1 and 5 μg/L, as can be observed in Table S2. Only BSA provided low recoveries (lower than 40%), whereas, the $\%R_{SPE}$ of the other compounds ranged from 71% to 92%.

After the procedure had been optimized using ultrapure water, the sorbent was tested with environmental water samples (river water, effluent wastewater, and influent wastewater). The apparent recoveries ($\%R_{app}$) obtained for 100 mL of river water adjusted to pH 3 and spiked at 5 μg/L, ranged from 58% to 78%. However, for effluent and influent wastewater samples, the $\%R_{app}$ for 100 mL ranged from 19% to 60%. The use of 50 mL was then tested, and the results were acceptable ($\%R_{app}$ between 49% and 76%). Thus, 100 mL was the volume selected for river samples and 50 mL for effluent and influent samples. Various loading volumes were selected for determining similar analytes: Asimakopoulos et al. selected 20 mL [38], Ajibola et al. 50 mL (effluent and influent) [6] and Hidalgo et al. 1 L (river and sea water) [7], although in this latter study the amount of sorbent was 500 mg. We considered that increasing of the loading volume was not needed due to the high sensitivity of LC-HRMS which provided low limits of detection. Moreover, if the loading volume had been increased, the amount of sorbent would have also been increased.

The elution volume of 5 mL of MeOH was evaporated to improve the sensitivity to around 150 μL and reconstituted to 1 mL of mobile phase. Evaporation to complete dryness was tested, but some compounds like the BTRs or Me-p-TSA suffered losses of about 30%, so evaporation was performed to about 150 μL to prevent analytes from being lost.

3.5. Validation of the method

Once the SPE procedure had been optimized, the method was validated according to the parameters described in section 2.6 that are apparent recovery calculated at two concentrations for river, effluent and influent wastewater samples, matrix effect, method detection (MDL) and quantification limits (MQL), repeatability and reproducibility between days. To calculate these parameters when necessary, the concentration of the blank was measured and subtracted from the signal of the spiked samples.

The $\%R_{app}$ was calculated after the river samples had been spiked at 1 and 5 μg/L (except for BSA and TSA which were spiked at 10 and 50 μg/L), and effluent and influent wastewater samples at 2 and 10 μg/L (except for BSA and TSA which were spiked at 20 and 100 μg/L). Spiking at lower concentrations was not evaluated because some of the compounds occurred naturally in the blank samples. Table 2 shows the $\%R_{app}$ obtained, which in most cases were above 50% (51%–85%), except for BSA (whose low recoveries have been pointed out before), OHBT in river samples (48%), and MeSBT (39%) and BTR (48%) in influent wastewater samples. These results are comparable with those reported in other studies [9,27] in which similar compounds were determined in

Table 1
Recoveries obtained when 25 mL of ultrapure water adjusted at pH 3 and 6 were percolated through SiO_2-G-SAX/SCX.

		pH 3	pH 6
BT	BT	107	105
	OHBT	91	92
	MeSBT	97	89
BTR	BTR	92	85
	5TTR	99	97
	4TTR	90	87
	ClBTR	85	81
	XTR	102	102
BSA	BSA	42	40
	TSA	78	75
	Me-p-TSA	95	73
	Et-p-TSA	90	87

Table 2
Apparent recoveries ($\%R_{app}$) when river, effluent and influent wastewater samples were spiked at two levels of concentration.

	River (100 mL)		Effluent WW (50 mL)		Influent WW (25 mL)	
Analyte	$\%R_{app}$ (1 μg/L)	$\%R_{app}$ (5 μg/L)	$\%R_{app}$ (2 μg/L)	$\%R_{app}$ (10 μg/L)	$\%R_{app}$ (2 μg/L)	$\%R_{app}$ (10 μg/L)
BT	52	43	53	53	64	71
OHBT	48	55	61	59	62	71
MeSBT	51	54	62	63	39	50
BTR	57	59	59	64	48	53
5TTR	53	56	68	72	64	63
4TTR	55	58	67	69	72	64
ClBTR	51	62	63	62	57	64
XTR	57	64	75	71	78	73
BSA	32	35	38	34	22	24
TSA	55	61	65	62	55	64
Me-p-TSA	64	65	77	75	70	74
Et-p-TSA	68	64	80	72	85	78

water with a commercial sorbent (Oasis HLB) to provide $\%R_{app}$ between 66% and 84% for river samples [27]. Another example was the use of a silica-based homemade sorbent to extract BTR, 5TTR, BT, OHBT and MeSBT, which gave recoveries between 70% and 114% in river samples [9].

Attending to the matrix effect (%ME), as can be observed in Fig. 5, in all cases (except for MeSBT) it was below ±30%. For influent wastewater samples, the signal of all the analytes was enhanced, and for river and effluent samples they were both suppression and enhancement of signal. All in all, excluding MeSBT, the %ME ranged from −19% to 30% for all analyzed samples. In particular, it should be pointed out that for BTRs the %ME was lower than ±20% even in influent wastewater samples. These results were remarkable since a clean-up step was not included to improve the selectivity of the method. The results were comparable to those obtained by other methods [11] which did contain a clean-up step, where the %ME ranged from −32% to +24% for the determination of similar compounds with commercial sorbents (Oasis MCX and MAX). In comparison with other studies without a selective clean-up step, the %ME was lower. For example, for the determination of BSA and TSA in effluent and influent wastewater samples with a commercial sorbent (Polyclean polymeric), %ME ranged from −40% to −65% [6]. In both cases, a polymer sorbent based on reversed phase interactions was used, while our sorbent was silica-based. Silica-based sorbents present lower non-specific interactions than polymer-based sorbents. In addition, since the interactions exploited in this article are the π-π ones thanks to the graphene, the selectivity of the extraction is enhanced.

MQLs and MDLs were also estimated from the instrumental limits and applying the recovery of each compound in each matrix. The results can be observed in Table S3, where MQL were lower than 18 ng/L in all cases except for BSA and TSA which, because of their high IQLs, were two orders of magnitude higher (300–900 ng/L). MDLs were lower than 10 ng/L in all cases except for BSA and TSA which were also considerably higher (154–455 ng/L). Several studies have reported similar MQLs and MDLs [6,9,11], for instance, Salas et al. [11] obtained MDLs in the range 10–42 ng/L and MQLs in the range 30–126 ng/L. Moreover, the high MDLs of BSA and TSA had been reported previously [7].

Both repeatability (% RSD, n = 4) and reproducibility between days (% RSD, n = 4) were lower than 18% for all analytes in all the matrixes.

3.6. Analysis of real samples

After the method had been validated, several river (Ebro), effluent wastewater and influent wastewater (Tarragona and Reus, Spain) samples were analyzed. Quantification was done by applying external calibration curves and using the apparent recoveries obtained previously. To confirm the occurrence of the compounds, the mass error of the molecular ion had to be lower than 5 ppm and the signal of at least one fragment ion had to be higher than 10^3 AU.

Table 3 shows the results obtained. In river samples, all BTs and BTRs were found in most samples. Only MeSBT, ClBTR and XTR were below the MQL in some samples since the signal of fragment ions did not reach 10^3 AU. BSAs were not detected except for few samples where Et-p-TSA could have been quantified. BT and OHBT were the compounds detected at the highest concentrations (175 and 104 ng/L, respectively). The highest levels of BT (150–500 ng/L) and XTR (370–1200 ng/L) were observed by Xu et al. [39] in waters from German rivers. Herrero et al. [27] and Hidalgo et al. [7] analyzed similar river samples and the concentration of BTRs was comparable. More specifically, Herrero et al. quantified 33–153 ng/L (BTR) and 26–69 ng/L (4TTR) [27] and Hidalgo

Table 3
Range of concentrations (ng/L) obtained after the analysis of river, effluent wastewater and influent wastewater samples through SPE/LC-HRMS using the SiO_2-G-SAX/SCX sorbent.

		River (n = 5)	Effluent WW (n = 5)	Influent WW (n = 5)
BT	BT	40–175	133–223	112–256
	OHBT	25–104	68–137	46–238
	MeSBT	<MQL - 18	<MQL	96–197
BTR	BTR	11–52	244–306	192–561
	5TTR	12–22	135–499	309–632
	4TTR	11–23	117–401	409–512
	ClBTR	<MQL - 12	MQL - 41	24–62
	XTR	<MQL - 11	MQL - 12	35–83
BSA	BSA	<MDL	<MDL	<MDL
	TSA	<MDL	<MDL	<MDL
	Me-p-TSA	<MDL	<MQL - 14	<MQL - 14
	Et-p-TSA	<MQL - 16	22–35	15–45

*RSD (%) < 15%. (n = 3).

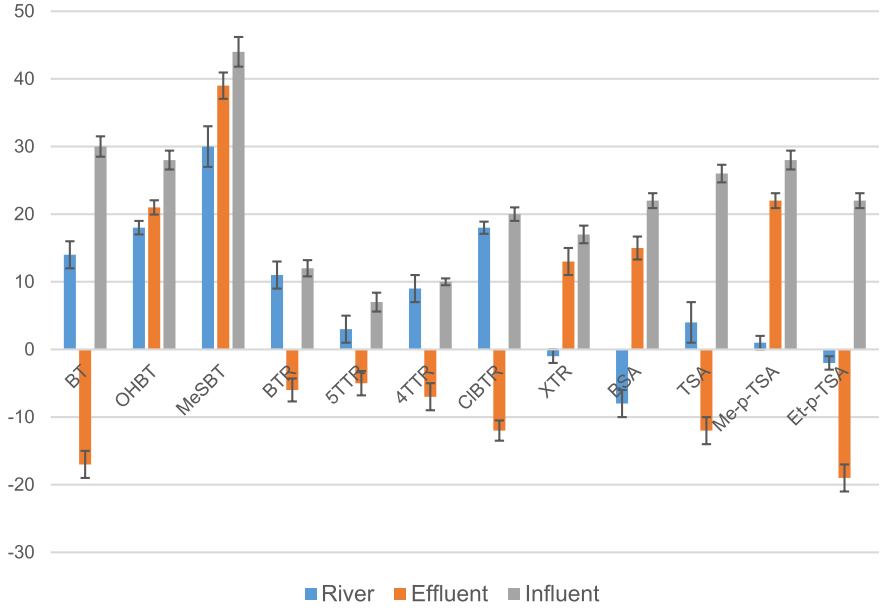

Fig. 5. Matrix effect obtained for each analyte in river, effluent and influent wastewater samples.

et al. quantified 34–78 ng/L (BTR) and 17–44 ng/L (4TTR) [7].

In wastewater samples, the compounds detected at highest concentrations were the BTRs, especially BTR, 4TTR and 5TTR in the influent wastewater samples which had concentrations around 500 ng/L. BSA and TSA were not detected due to their high detection limits, but Me-p-TSA and Et-p-TSA were detected in all samples and quantified in most of them. In general, the concentrations in influent wastewater samples were higher than in effluent wastewater, which suggests that these compounds had been partially removed in wastewater treatment plants. Salas et al. [11] determined BTs and BTRs in effluent and influent wastewater samples: the levels of BTs were similar (243–358 ng/L in effluent wastewater samples and 286–767 ng/L in influent wastewater samples) but BTRs were significantly higher (4TTR ranged from 666 to 1697 ng/L in effluent samples and from 743 to 1236 ng/L in influent wastewater samples). Dominguez et al. [40] found similar concentrations in effluent and influent wastewater samples. Concentrations of BT were close to 250 ng/L, which were similar to the concentrations found in the present study (112–256 ng/L).

BSA and TSA were not detected due to their high detection limits. Moreover, the other BSAs were found in low concentrations (<45 ng/L) in the samples.

4. Conclusions

A novel mixed-mode zwitterionic sorbent based on a silica network modified with graphene microparticles was synthesized. The sol-gel synthesis provided a facile pathway to molecular level integration of organic/inorganic polymer, organically modified sol-gel precursors as well as high surface area carbonaceous particles. The sol-gel synthesis maximizes the available surface area of the carbonaceous particles. In the current study, graphene with its high surface area and inherent capability to exert π-π interactions towards the analytes complements to the overall selectivity of the resulting SiO_2-G-SAX/SCX sorbent.

The sorbent was successfully applied for the extraction of a group of BTs, BTRs and BSAs. During the optimization of the sorbent, it was observed that the analytes were mainly retained in the sorbent through π-π interactions and various SPE parameters were optimized to exploit these interactions.

A method was successfully developed to determine the group of BTs, BTRs and BSAs in river, effluent wastewater, and influent wastewater samples using SPE followed by LC-HRMS. The results in terms of matrix effect were extremely low, considering that there was no clean-up step to improve the selectivity. These results suggest that this sorbent can be evaluated with other compounds with which π-π interactions can be performed.

Credit author

Alberto Moral, Investigation, Resources, Validation, Writing original draft. Francesc Borrull, Supervision, Funding acquisition. Kenneth G. Furton, Supervison, Conceptualization. Abuzar Kabir, Project Administration, Conceptualization, Methodology. Núria Fontanals, Project Administration, Conceptualization, Writing original draft. Rosa Maria Marcé, Methodology, Writing, Review and Editing.

Declaration of competing interest

The authors declare that they have no known competing financial interests or personal relationships that could have appeared to influence the work reported in this paper.

Data availability

Data will be made available on request.

Acknowledgements

The authors wish to acknowledge the financial support provided by the grant PID2020-114587 GB-100 and RED2018-102522-T funded by MCIN/AEI/10.12039/501100011033 and by "ERDF A way making Europe. The author also acknowledged the University Rovira i Virgili (URV) for his PhD grant (2020PMF-PIPF-33).

Appendix A. Supplementary data

Supplementary data to this article can be found online at https://doi.org/10.1016/j.talanta.2023.124315.

References

[1] S.D. Richardson, S.Y. Kimura, Emerging environmental contaminants: challenges facing our next generation and potential engineering solutions, Environ. Technol. Innovat. 8 (2017) 40–56, https://doi.org/10.1016/j.eti.2017.04.002.
[2] W. Vetter, J. Lorenz, Determination of benzotriazoles in dishwasher tabs from Germany and estimation of the discharge into German waters, Environ. Sci. Pollut. Res. 20 (2013) 4435–4440, https://doi.org/10.1007/s11356-012-1386-y.
[3] Z.Q. Shi, Y.S. Liu, Q. Xiong, W.W. Cai, G.G. Ying, Occurrence, toxicity and transformation of six typical benzotriazoles in the environment: a review, Sci. Total Environ. 661 (2019) 407–421, https://doi.org/10.1016/j.scitotenv.2019.01.138.
[4] A. Naccarato, A. Tassone, M. Martino, R. Elliani, F. Sprovieri, N. Pirrone, A. Tagarelli, An innovative green protocol for the quantification of benzothiazoles, benzotriazoles and benzosulfonamides in PM10 using microwave-assisted extraction coupled with solid-phase microextraction gas chromatography tandem-mass spectrometry, Environ. Pollut. 285 (2021), 117487, https://doi.org/10.1016/j.envpol.2021.117487.
[5] C. Liao, U.J. Kim, K. Kannan, A review of environmental occurrence, fate, exposure, and toxicity of benzothiazoles, Environ. Sci. Technol. 52 (2018) 5007–5026, https://doi.org/10.1021/acs.est.7b05493.
[6] A. Ajibola, P. Gago-Ferrero, V.L. Borova, M.E. Dasenaki, A.A. Bletsou, N. S. Thomaidis, Benzosulfonamides in wastewater: method development, occurrence and removal efficiencies, Chemosphere 119 (2015) S21–S27, https://doi.org/10.1016/j.chemosphere.2014.04.003.
[7] M. Hidalgo-Serrano, F. Borrull, R.M. Marcé, E. Pocurull, Presence of benzotriazoles, benzothiazoles and benzenesulfonamides in surface water samples by liquid chromatography coupled to high-resolution mass spectrometry, Sep. Sci. Plus. 2 (2019) 72–80, https://doi.org/10.1002/sscp.201800140.
[8] W. Xu, W. Yan, T. Licha, Simultaneous determination of trace benzotriazoles and benzothiazoles in water by large-volume injection/gas chromatography-mass spectrometry, J. Chromatogr. A 1422 (2015) 270–276, https://doi.org/10.1016/j.chroma.2015.10.017.
[9] A. Speltini, M. Pastore, F. Merlo, F. Maraschi, M. Sturini, D. Dondi, A. Profumo, Humic acids pyrolyzed onto silica microparticles for solid-phase extraction of benzotriazoles and benzothiazoles from environmental waters, Chromatographia 82 (2019) 1275–1283, https://doi.org/10.1007/s10337-019-03699-9.
[10] A. Speltini, F. Maraschi, M. Sturini, M. Contini, A. Profumo, Dispersive multi-walled carbon nanotubes extraction of benzenesulfonamides, benzotriazoles, and benzothiazoles from environmental waters followed by microwave desorption and HPLC-HESI-MS/MS, Anal. Bioanal. Chem. 409 (2017) 6709–6718, https://doi.org/10.1007/s00216-017-0627-9.
[11] D. Salas, F. Borrull, R.M. Marcé, N. Fontanals, Study of the retention of benzotriazoles, benzothiazoles and benzenesulfonamides in mixed-mode solid-phase extraction in environmental samples, J. Chromatogr. A 1444 (2016) 21–31, https://doi.org/10.1016/j.chroma.2016.03.053.
[12] P. Herrero, F. Borrull, E. Pocurull, R.M. Marcé, An overview of analytical methods and occurrence of benzotriazoles, benzothiazoles and benzenesulfonamides in the environment, TrAC, Trends Anal. Chem. 62 (2014) 46–55, https://doi.org/10.1016/j.trac.2014.06.017.
[13] A. Maceira, R.M. Marcé, F. Borrull, Occurrence of benzothiazole, benzotriazole and benzenesulfonamide derivates in outdoor air particulate matter samples and human exposure assessment, Chemosphere 193 (2018) 557–566, https://doi.org/10.1016/j.chemosphere.2017.11.073.
[14] C. Yang, S. He, S. Lu, X. Liao, Y. Song, Z.F. Chen, G. Zhang, R. Li, C. Dong, Z. Qi, Z. Cai, Pollution characteristics, exposure assessment and potential cardiotoxicities of PM2.5-bound benzotriazole and its derivatives in typical Chinese cities, Sci. Total Environ. 809 (2022), 151132, https://doi.org/10.1016/j.scitotenv.2021.151132.
[15] C.H. Chen, W.H. Chung, W.H. Ding, Determination of benzotriazole and benzothiazole derivatives in marketed fish by double-vortex-ultrasonic assisted matrix solid-phase dispersion and ultrahigh-performance liquid chromatography-high resolution mass spectrometry, Food Chem. 333 (2020), 127516, https://doi.org/10.1016/j.foodchem.2020.127516.
[16] J. Li, H. Zhao, Y. Zhou, S. Xu, Z. Cai, Determination of benzotriazoles and benzothiazoles in human urine by UHPLC-TQMS, J. Chromatogr. B 1070 (2017) 70–75, https://doi.org/10.1016/j.jchromb.2017.10.045.
[17] R. Avagyan, I. Sadiktsis, G. Thorsén, C. Östman, R. Westerholm, Determination of benzothiazole and benzotriazole derivates in tire and clothing textile samples by high performance liquid chromatography-electrospray ionization tandem mass

spectrometry, J. Chromatogr. A 1307 (2013) 119–125, https://doi.org/10.1016/j.chroma.2013.07.087.
[18] W. Liu, J. Xue, K. Kannan, Occurrence of and exposure to benzothiazoles and benzotriazoles from textiles and infant clothing, Sci. Total Environ. 592 (2017) 91–96, https://doi.org/10.1016/j.scitotenv.2017.03.090.
[19] C.J. Hsu, W.H. Ding, Determination of benzotriazole and benzothiazole derivatives in tea beverages by deep eutectic solvent-based ultrasound-assisted liquid-phase microextraction and ultrahigh-performance liquid chromatography-high resolution mass spectrometry, Food Chem. 368 (2022), 130798, https://doi.org/10.1016/j.foodchem.2021.130798.
[20] H. Kim, B. Kim, Y. Shin, J. Kim, H. Kim, K. Kim, P. Kim, K. Park, Comparative Biochemistry and Physiology , Part C Effect of benzotriazole on oxidative stress response and transcriptional gene expression in Oryzias latipes and Danio rerio embryo, Comp. Biochem. Physiol., C 252 (2022), 109222, https://doi.org/10.1016/j.cbpc.2021.109222.
[21] X. Liang, C.J. Martyniuk, J. Zha, Z. Wang, Brain quantitative proteomic responses reveal new insight of benzotriazole neurotoxicity in female Chinese rare minnow (Gobiocypris rarus), Aquat. Toxicol. 181 (2016) 67–75, https://doi.org/10.1016/j.aquatox.2016.10.030.
[22] X. Chen, Y. Zhou, C. Hu, W. Xia, S. Xu, Z. Cai, Y. Li, Prenatal exposure to benzotriazoles and benzothiazoles and cord blood mitochondrial DNA copy number: a prospective investigation, Environ. Int. 143 (2020), 105920, https://doi.org/10.1016/j.envint.2020.105920.
[23] W. Li, J. Li, M. Deng, Y. Pan, L. Zeng, Benzotriazoles and benzothiazoles prevail in indoor dust from an E-waste dismantling area in South China: elevated concentrations and implication for human exposure, Sci. Total Environ. 723 (2020), 137979, https://doi.org/10.1016/j.scitotenv.2020.137979.
[24] R. Meffe, C. Kohfahl, E. Hamann, Fate of para-toluenesulfonamide (p-TSA) in groundwater under anoxic conditions : modelling results from a field site in Berlin (Germany), Environ. Sci. Pollut. Res. 21 (2014) 568–583, https://doi.org/10.1007/s11356-013-1902-8.
[25] E.N.F.L. Canova, M. Sturini, F. Maraschi, S. Sangiorgi, A comparative test on the sensitivity of freshwater and marine microalgae to benzo-sulfonamides, -thiazoles and -triazoles, Appl. Sci. 11 (2021) 7800, https://doi.org/10.3390/app11177800.
[26] D. Richter, G. Massmann, T. Taute, U. Duennbier, Investigation of the fate of sulfonamides downgradient of a decommissioned sewage farm near Berlin , Germany, J. Contam. Hydrol. 106 (2009) 183–194, https://doi.org/10.1016/j.jconhyd.2009.03.001.
[27] P. Herrero, F. Borrull, E. Pocurull, R.M. Marcé, Efficient tandem solid-phase extraction and liquid chromatography-triple quadrupole mass spectrometry method to determine polar benzotriazole, benzothiazole and benzenesulfonamide contaminants in environmental water samples, J. Chromatogr. A 1309 (2013) 22–32, https://doi.org/10.1016/j.chroma.2013.08.018.
[28] V. Osorio, M. Schriks, D. Vughs, P. de Voogt, A. Kolkman, A novel sample preparation procedure for effect-directed analysis of micro-contaminants of emerging concern in surface waters, Talanta 186 (2018) 527–537, https://doi.org/10.1016/j.talanta.2018.04.058.
[29] I. Carpinteiro, B. Abuin, M. Ramil, I. Rodríguez, R. Cela, Simultaneous determination of benzotriazole and benzothiazole derivatives in aqueous matrices by mixed-mode solid-phase extraction followed by liquid chromatography-tandem mass spectrometry, Anal. Bioanal. Chem. 402 (2012) 2471–2478, https://doi.org/10.1007/s00216-012-5718-z.
[30] J.C. Nadal, S. Dargo, F. Borrull, P.A.G. Cormack, N. Fontanals, R.M. Marcé, Hypercrosslinked polymer microspheres decorated with anion- and cation-exchange groups for the simultaneous solid-phase extraction of acidic and basic analytes from environmental waters, J. Chromatogr. A 1661 (2022), 462715, https://doi.org/10.1016/j.chroma.2021.462715.
[31] J.C. Nadal, K.L. Anderson, S. Dargo, I. Joas, D. Salas, F. Borrull, P.A.G. Cormack, R. M. Marcé, N. Fontanals, Microporous polymer microspheres with amphoteric character for the solid-phase extraction of acidic and basic analytes, J. Chromatogr. A 1626 (2020), 461348, https://doi.org/10.1016/j.chroma.2020.461348.
[32] A. Moral, F. Borrull, K.G. Furton, A. Kabir, N. Fontanals, R. Maria, Development of sol-gel silica-based mixed-mode zwitterionic sorbents for determining drugs in environmental water samples, J. Chromatogr. A 1676 (2022), 463237, https://doi.org/10.1016/j.chroma.2022.463237.
[33] S. Jin, Y. Qiao, J. Xing, Ternary mixed-mode silica sorbent of solid-phase extraction for determination of basic, neutral and acidic drugs in human serum, Anal. Bioanal. Chem. 410 (2018) 3731–3742, https://doi.org/10.1007/s00216-018-1037-3.
[34] E. Vasconcelos, S. Maciel, A. Lúcia, D. Toffoli, E. Sobieski, C. Eduardo, D. Nazario, F. Mauro, Materials in sample preparation : recent advances and future trends, Trends Anal. Chem. 119 (2019), 115633, https://doi.org/10.1016/j.trac.2019.115633.
[35] W. Jing, J. Wang, B. Kuipers, W. Bi, D.D.Y. Chen, Recent applications of graphene and graphene-based materials as sorbents in trace analysis, TrAC, Trends Anal. Chem. 137 (2021), 116212, https://doi.org/10.1016/j.trac.2021.116212.
[36] N. Ye, P. Shi, Applications of graphene-based materials in solid-phase extraction and solid-phase microextraction, Separ. Purif. Rev. 44 (2015) 183–198, https://doi.org/10.1080/15422119.2014.912664.
[37] I.O. Faniyi, O. Fasakin, B. Olofinjana, A.S. Adekunle, T.V. Oluwasusi, M.A. Eleruja, E.O.B. Ajayi, The comparative analyses of reduced graphene oxide (RGO) prepared via green, mild and chemical approaches, SN Appl. Sci. 1 (2019) 1181, https://doi.org/10.1007/s42452-019-1188-7.
[38] A.G. Asimakopoulos, A.A. Bletsou, Q. Wu, N.S. Thomaidis, K. Kannan, Determination of benzotriazoles and benzothiazoles in human urine by liquid chromatography-tandem mass spectrometry, Anal. Chem. 85 (2013) 441–448, https://doi.org/10.1021/ac303266m.
[39] I. Kraševec, H. Prosen, Determination of polar benzotriazoles in aqueous environmental samples by hollow-fibre microextraction method with LC-MS/MS and its comparison to a conventional solid-phase extraction method, Microchem. J. 166 (2021), 106191, https://doi.org/10.1016/j.microc.2021.106191.
[40] C. Domínguez, C. Reyes-Contreras, J.M. Bayona, Determination of benzothiazoles and benzotriazoles by using ionic liquid stationary phases in gas chromatography mass spectrometry. Application to their characterization in wastewaters, J. Chromatogr. A 1230 (2012) 117–122, https://doi.org/10.1016/j.chroma.2012.01.054.